Korea-Australia Rheology Journal
Vol. 20, No. 1, March 2008 pp. 15-26

An instability criterion for viscoelastic flow past a confined cylinder

Hua-Shu Dou[1,*] and Nhan Phan-Thien[2]
[1]*Temasek Laboratories, The National University of Singapore, Singapore 117508*
[2]*Department of Mechanical Engineering, The National University of Singapore, Singapore 119260*
(Received Nov. 28, 2007; final revision received Jan. 20, 2008)

Abstract

It has been known that there is a viscoelastic instability in the channel flow past a cylinder at high Deborah (*De*) number. Some of our numerical simulations and a boundary layer analysis indicated that this instability is related to the shear flow in the gap between the cylinder and the channel walls in our previous work. The critical condition for instability initiation may be related to an inflection velocity profile generated by the normal stress near the cylinder surface. At high *De*, the elastic normal stress coupling with the streamline curvature is responsible for the shear instability, which has been recognized by the community. In this study, an instability criterion for the flow problem is proposed based on the analysis on the pressure gradient and some supporting numerical simulations. The critical *De* number for various model fluids is given. It increases with the geometrical aspect ratio *h/R* (half channel width/cylinder radius) and depends on a viscosity ratio β (polymer viscosity/total viscosity) of the model. A shear thinning first normal stress coefficient will delay the instability. An excellent agreement between the predicted critical Deborah number and reported experiments is obtained.

Keywords : instability, criterion, viscoelastic, normal stress, curvature, flow past a cylinder

1. Introduction

Purely viscoelastic instabilities at high Deborah numbers have attracted a considerable interest in the literature, for example, Larson (1992), Shaqfeh (1996), McKinley *et al.* (1996), and Wilson (2006). Understanding these instabilities which occur at low speed is meaningful from the academic interests. Furthermore, these instabilities appear in a number of polymer processes and therefore also have practical significance.

Most viscoelastic instability studies concentrate on simple geometry, such as coaxial plates, cone-and-plate devices, and Couette and Poiseuille flows. Few were done for complex geometry, *e.g.*, the torsional instability in a finite domain (Avagliano and Phan-Thien, 1998) and the instability for the flow past a confined cylinder (McKinley *et al.*, 1993). In the latter, McKinley *et al.* (1993) demonstrated for the flow past a confined cylinder, an instability first appears in the cylinder wake, near the rear stagnation point and is convected downstream. When the Deborah number is beyond a certain value, a large downstream shift in the velocity profile is generated progressively. With further increasing in the *De* number beyond a critical value, the steady planar stagnation flow in the downstream wake becomes a three-dimensional cellular structure. There are large spatially periodic fluctuations in the streamwise velocity extending along the length of the cylinder in the wake region close to the cylinder. At still a higher *De* number, the flow becomes a *steady* translation of the cellular structure along the length of the cylinder and time-dependent velocity oscillations are observed in the wake. The mechanism of instability in the cylinder wake is poorly understood (Larson, 1992). Byars (1996) (see also Smith *et al.*, 2000) had reported a transition from the two-dimensional base flow to a three-dimensional cellular structure in the cylinder wake. At a higher Deborah number, the instability extends to the upstream of the wake and appears in the shear layer on the cylinder surface. Shiang *et al.* (2000)'s experiments for viscoelastic flow past a confined cylinder showed the similar behavior which the viscoelastic flow bifurcates from steady two-dimensional flow to steady three-dimensional flow for values of Deborah number greater than a critical value. These elastic instabilities do not exist in the Newtonian counterpart of creeping flow past a cylinder. Larson *et al.* (1990) suggested that the mechanism of instability in viscoelastic flows with curved streamlines is due to the coupling of a perturbation radial extensional flow to the base-state stress gradients leading to a perturbation in the non-Newtonian "hoop stress" $\tau_{\theta\theta}$. This perturbation is then able to induce a secondary flow in the cross-flow direction of the base flow streamlines. Based on the elastic instability due to

*Corresponding author: tsldh@nus.edu.sg, huashudou@yahoo.com

normal stresses in curved streamlines, McKinley *et al.* (1996) proposed a general instability criterion using an equivalent radius of curvature for various geometry, which can be thought of as the viscoelastic analogue of the Görtler number.

We found that there is a similarity of the instabilities occurred in viscoelastic and Newtonian flows. We discovered that the energy gradient may link to instability in both types of flows and a theory has been proposed. We believe that the principle of this theory is universal for the flow instabilities in both Newtonian and non-Newtonian flows. In this theory, any disturbance amplification is considered as the evolution of the disturbance energy driven by the energy gradient of the main flow. Large energy gradient may lead to a larger disturbance amplification and a small energy gradient may not be able to provide sufficient energy to increase the disturbance energy. Dou (2006a) showed that the gradient of total energy in the transverse direction of the main flow and the energy loss due to viscous friction in the streamwise direction dominate the instability phenomena, and hence the critical condition of flow instability for a given disturbance. The analysis was consistent with results for plane and pipe Poiseuille flows, and plane Couette flow for Newtonian fluid at the critical condition (Dou, 2006a). It was also demonstrated that an inflection point for the velocity profile is a sufficient, but not a necessary condition, for flow instability, for both inviscid and viscous flows. Therefore, any flows with an inflectional velocity profile are unstable. One should note that necessary condition and sufficient condition are very different for a given problem. Later, Dou (2006b, 2007) carried out detailed derivations to support this theory (named as *energy gradient theory*), and explained recent modern experimental results about the scaling of the threshold of disturbance amplitude with Reynolds number in the literature. Now, this theory has been applied to Taylor-Couette flows between concentric rotating cylinders (Dou *et al.*, 2007). Since the mechanism of flow instability in this theory only depends on the energy distribution in the flow field (under a given disturbance), the principle of instability is believed to be applicable to the case of viscoelastic flows.

For the viscoelastic flow past a confined cylinder (Fig. 1), simulations had been carried out with a variety of differential constitutive models, including the Upper Convected Maxwell (UCM), the Phan-Thien-Tanner (PTT), the Oldroyd-B, the Giesekus, the FENE-CR (Finitely Extensible Nonlinear Elastic-Chilcott-Rallison), and also the K-BKZ integral models (see a short review in Dou and Phan-Thien, 1999; Dou and Phan-Thien, 2007). Recently, Dou and Phan-Thien (2007) found that the flow instability may be related to a velocity inflection near the cylinder at high *De* due to normal stress effect. A simulation of a Boger fluid with viscosity ratio β=0.41, and channel half width

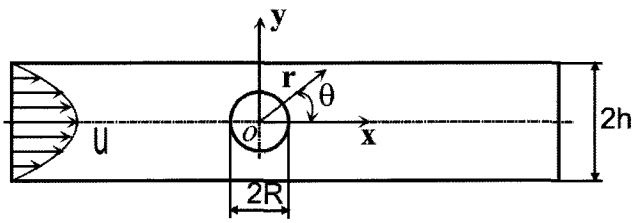

Fig. 1. Schematic diagram of the flow around a cylinder in a channel.

to cylinder radius ratio h/R=2, using a single-mode Oldroyd-B model (McKinley *et al.*, 1993) indicated that a velocity inflection appeared at a critical Deborah number of $De \sim 0.6$. This velocity inflection may lead to flow instability and amplify any disturbance in the kinematics as the way in Newtonian flows, according to the newly proposed theory (Dou, 2004; Dou, 2006a; Dou, 2006b). They thought that the flow instability was caused by shear on the cylinder rather than elongation in the wake (Dou and Phan-Thien, 2007).

This paper is a successor of our work in a separate publication (Dou and Phan-Thien, 2007). In Dou and Phan-Thien (2007), we presented the numerical simulation and boundary-layer analysis results, and gave an explanation of the mechanism of instability. In present paper, a viscoelastic flow instability criterion is proposed based on boundary layer analysis and simulation results. The critical *De* number for a viscoelastic flows past a cylinder in a channel is given. The results show that the critical *De* number increases with the aspect ratio h/R and is of $O(\beta^{-1/2})$. Only constant viscosity fluids are considered here, using differential constitutive equations such as UCM, Oldroyd-B, and FENE-CR models. Comparison of the prediction to the experimental data in literature is made.

2. Governing equations

The equations of mass, momentum conservation, and the constitutive equations for the UCM, Oldroyd-B, Phan-Thien-Tanner (PTT with affine motion), and FENE-CR models are (Bird *et al.*, 1987; Huilgol and Phan-Thien, 1997):

$$\nabla \cdot \mathbf{u} = 0 \quad \text{(incompressibility)}, \tag{1}$$

$$\rho\left(\frac{\partial \mathbf{u}}{\partial t} + \mathbf{u} \cdot \nabla \mathbf{u}\right) = -\nabla p + \nabla \cdot \boldsymbol{\tau} + \eta_N \nabla^2 \mathbf{u} \quad \text{(momentum)}, \tag{2}$$

$$g\boldsymbol{\tau} + \lambda\left\{\frac{\partial}{\partial t}\left(\frac{\boldsymbol{\tau}}{f}\right) + \mathbf{u} \cdot \nabla\left(\frac{\boldsymbol{\tau}}{f}\right) - \nabla \mathbf{u}^T \cdot \left(\frac{\boldsymbol{\tau}}{f}\right) - \left(\frac{\boldsymbol{\tau}}{f}\right) \cdot \nabla \mathbf{u}\right\} = 2\eta_{m0}\mathbf{D}$$

(constitutive), (3)

$$g = 1 + \frac{\varepsilon\lambda}{\eta_{m0}} tr\boldsymbol{\tau}, \tag{4}$$

$$f=\left(1-\frac{e}{L^2}\frac{3+\frac{\lambda}{\eta_{m0}}tr\tau}{1+\left(\frac{\lambda}{\eta_{m0}}tr\tau\right)/L^2}\right)^{-1}, \quad (5)$$

where ρ is the fluid density, t the time, $\mathbf{u}$ the velocity vector, p the hydrodynamic pressure, $\eta_N\nabla^2\mathbf{u}$ the contribution from a Newtonian stress tensor, with η_N a "solvent" viscosity, $\mathbf{D}=(\nabla\mathbf{u}+\nabla\mathbf{u}^T)/2$ is the rate-of-strain tensor, η_{m0} a "polymer-contributed" viscosity, λ the (constant) relaxation time, ε a dimensionless parameter, $tr\tau$ the trace of tensor τ, τ the "extra" stress tensor from the contribution of viscoelastic stress (not necessarily traceless), L is the maximum extension length of dumbbells, and e is a parameter. For PTT, UCM and Oldroyd-B models, $e=0$; for the FENE-CR model $e=1$. If the solvent viscosity $\eta_N=0$, the equations describe a general flow of the PTT fluid. If $\eta_N=0$, and $\varepsilon=0$, the Upper Convected Maxwell (UCM) model is recovered. When $\varepsilon=0$, the system reduces to the Oldroyd-B model or the FENE-CR model. If the relaxation time λ is set to zero, the Newtonian fluid case is recovered, with viscosity $\eta_0=\eta_N+\eta_{m0}$; this is also the viscosity of the fluid. The total stress tensor is the sum, $\tau_t=\tau_N+\tau=2\eta_N\mathbf{D}+\tau$.

By dening $\beta=\eta_{m0}/\eta_0$ as the retardation ratio, we have $\eta_N=\eta_0(1-\beta)$. For UCM and PTT models, $\beta=1$, and $\eta_0=\eta_{m0}$. For the Newtonian fluid, $\beta=0$, and $\eta_0=\eta_N$. For the Oldroyd-B and FENE-CR fluids, $0<\beta<1$, and $\eta_0=\eta_{m0}/\beta$. The rheological behaviours of these constitutive models were discussed in detail by Bird *et al.* (1987) and Huilgol and Phan-Thien (1997).

3. Observations from simulation results

In this problem, the Deborah number, $De=\lambda U/R$, is defined based on the average velocity U in the channel, and the radius R of the cylinder. Only creeping flow is considered ($\mathrm{Re}=\rho UR/\eta_0=0$). In our previous work (Dou and Phan-Thien, 2007), the numerical method used for the simulation of viscoelastic flows is described in detail. It employed the DEVSS-ω scheme and an unstructured finite volume method.

The computing domain is generally shown in Fig. 1. The boundary conditions for the numerical solution are briefly stated here. The flows at the inlet and outlet are assumed to be fully developed Poiseuille flow, with the boundary conditions for u, v, and for τ_{xx}, τ_{xy} and τ_{yy} as given by analytical solutions. No-slip conditions are also imposed for u, v on solid surfaces. On these, τ_{xx}, τ_{xy} and τ_{yy} are calculated by using the current velocity gradient at each iteration level. In principle, the stress boundary conditions at the downstream boundary are unnecessary. However, giving correct boundary values at these nodes can speed up the convergence, provided that the downstream is sufficient for the stresses to be fully developed. The details are described in Dou and Phan-Thien (1999, 2007).

Extensive simulations were carried out for the MIT 0.31 wt%PIB Boger fluid (relaxation time $\lambda=0.794$ s, viscosity ratio $\beta=0.41$) (McKinley *et al.*, 1993) with $h/R=2$, using a single-mode Oldroyd-B model. Simulations using fine, thin and long triangle meshes ($\Delta r/R<0.04$, $\Delta r/\Delta s=0.30$) indicates that a velocity inflection on the cylinder surface at plane $x=0$ appears at a critical De number ($De\sim 0.6$) (Dou and Phan-Thien, 2007). The appearance of the inflection point in the velocity profile is related to the pressure distribution in the normal direction from the cylinder. It has been found that for Newtonian flow, the pressure distribution along the plane $x=0$ is uniform and the velocity gradient distribution along the plane $x=0$ is linear. At low De number ($De<0.6$), although the pressure within the shear layer is higher than that outside, the velocity gradient is still nearly linear, and hence a parabolic velocity distribution results. At high De number ($De>0.6$), the pressure within the shear layer is much higher than that outside ($\partial p/\partial y$ is large along $x=0$). The maximum in the velocity gradient appears, and with it, the inflection point in the velocity profile is formed. This is because the pressure gradient $\partial p/\partial y$ forces the normal velocity of fluid particles near the wall to increase, and finally leads to the inflection. We believe that the instability is induced by this velocity inflection according to the recent proposed energy gradient theory (Dou, 2006a; Dou, 2006b). The critical De number for the appearance of inflection velocity found in Oldroyd-B fluid simulation ($De\sim 0.60$) is also near the experimental value found by Byars (1996) (see also Smith *et al.*, 2000). The velocity, velocity gradient, and pressure distributions can be sketched as in Fig. 2 for different De numbers.

Recently, we simulated the flow with the FENE-CR model ($\beta=0.41$, $L=12$), using the same conditions and the same mesh, the velocity inflection appears at the about same De number ($De=0.65$).

Caola *et al.* (2001)' s simulation results also showed that the velocity gradient on the top of the cylinder deviates from the Newtonian flow with the increasing De in the range of $r/R<1.1$ and tends to generate an inflection near the cylinder (Fig. 12 in Caola *et al.*, 2001). This result is in agreement with ours.

The normal stress $\tau_{\theta\theta}$ increases on the first half cylinder and decreases on the second half. It reaches maximum at the position near plane $x=0$ where p is subjected to most severe pressure distortions due to thin boundary layer and flow changes from acceleration to deceleration (the latter factor is negligible for $Re\sim 0$). Thus, the inflection in velocity profile may be induced easier there.

Another supporting evidence for the present study is the limiting De number obtained by the simulation of steady flows. Studies for an Oldroyd-B fluid in reference (Dou and Phan-Thien, 2007) showed that the limiting De num-

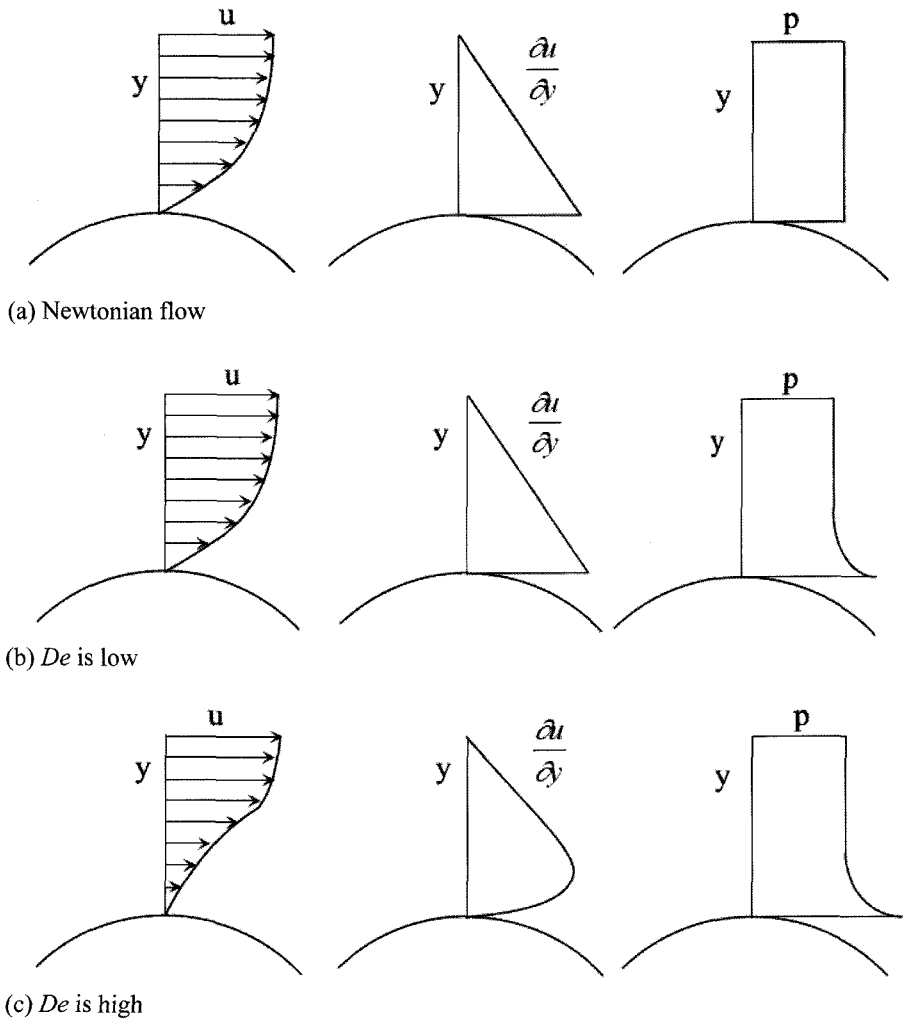

Fig. 2. Schematic diagrams of velocity, velocity gradient, and pressure on the cylinder along $x=0$.

ber obtained by simulations is related to the aspect ratio of meshes. The most useful informations provided by simulations are those obtained with refined meshes ($\Delta r/R$ should be comparable to the thickness of stress boundary layer). In this study, it should be $\Delta r/R<0.04$ in order to obtain the picture of the real flow near the cylinder surface (see Dou and Phan-Thien, 2007). Using thin and long triangle meshes ($\Delta r/\Delta s=0.30$), the convergent solution of steady flows breaks down at about $De=1.1$ for the studied Oldroyd-B fluid. This is in agreement with the most simulation results in the literature (see Dou and Phan-Thien, 1999; Caola *et al.*, 2001). However, when we use equilateral triangle meshes ($\Delta r/\Delta s=0.70$), the convergent solution of steady flows breaks down at about $De=0.60$, and meanwhile a tendency of velocity inflection appears. As we know, thin and long triangle meshes try to amplify the discretization error and to stabilize the computation. This could delay the breakdown of steady solutions. Equilateral triangle meshes tend to give more exact solution of the dependent variables. Any exact steady flow solution should break down at a *De* number at which the flow instability sets in. This means that $De=0.60$ is the critical Deborah number (De_c) for flow instability initiation for the used Oldroyd-B fluid. This result coincides with instability margin given by the velocity inflection appearance. Thin and long triangle meshes could pass through this margin is due to the more stability of the thin meshes for the numerical process. Any steady simulation results beyond De_c could not represent the physical flow of the fluid. Therefore, it is no sense to pursue a high *De* number solution for steady flow beyond De_c in the high Deborah flow problems. This result about the effect of aspect ratio of meshes is consistent with the results of linear stability analysis (Smith *et al.*, 2000).

Most simulation results in the literature showed that numerical convergence at centerline has been achieved for $De=0.7-0.8$ for the cylinder problem (Poiseuille flow) with Oldroyd-B or UCM fluids (see Dou and Phan-Thien, 2007). In addition, the stress gradients in the cylinder wake may be numerically unbounded at *De* of $O(1)$. More

recently, Kim *et al.* (2004) obtained a convergence Deborah number of $De=0.7$ using a high order scheme. In their computing, they used meshes with aspect ratio of about 1. Hulsen *et al.* (2005) showed that a convergence Deborah number of $De=0.6$ was achievable and that the problem of numerical convergence was not resolved. Oliveira and Miranda (2005) claimed that the flow was already separated at a Deborah number of $De=1.0$. Thus, from these numerical results, it appears that a reliable value of the Deborah number at convergence is only about 0.6~0.7.

In the following section, the velocity inflection condition ($De=0.60$) is only taken as an additional evidence for the scaling of critical condition of instability. The idea in our criterion is the pressure gradient in the transverse direction which leads to secondary flow along the radial (transversal) direction. This secondary flow inevitably results in a tendency of less full velocity profile, and a tendency of inflection. We used the pressure gradient magnitude to establish the criterion, and used above-mentioned $De_c=0.6$ to set up a value of critical condition. This value is supported by the following facts. (a) The exact solution of steady flows breaks down at $De=0.6$ in numerical simulations (equilateral triangular meshes). (b) The critical value $De=0.6$ is agreement with Byars's experimental data (Byars, 1996). In practical flows, the development of instability depends on the level of disturbance in the flows. If the disturbance is very small, the instability may be difficult to spread downstream; or at same level of disturbance, the instability can only be amplified at a higher De number.

4. Proposed instability criterion

4.1. Flow instability initiation

In the following analysis, we use u, v to denote the Cartesian components, and u_θ, u_r the polar components of the velocity vector. In cylindrical coordinates, the steady momentum equations are

$$\rho\left(\frac{u_\theta}{r}\frac{\partial u_\theta}{\partial\theta}+u_r\frac{\partial u_\theta}{\partial r}\right)=-\frac{1}{r}\frac{\partial p}{\partial\theta}-\rho\frac{u_\theta u_r}{r}+\frac{1}{r^2}\frac{\partial}{\partial r}(r^2\tau_{r\theta})+\frac{1}{r}\frac{\partial\tau_{\theta\theta}}{\partial\theta}, \quad (6)$$

$$\rho\left(\frac{u_\theta}{r}\frac{\partial u_r}{\partial\theta}+u_r\frac{\partial u_r}{\partial r}\right)=-\frac{\partial p}{\partial r}+\rho\frac{u_\theta^2}{r}+\frac{1}{r}\frac{\partial}{\partial r}(r\tau_{rr})-\frac{\tau_{\theta\theta}}{r}+\frac{1}{r}\frac{\partial\tau_{r\theta}}{\partial\theta}. \quad (7)$$

The stresses in above equations are the total stresses. For creeping flows, the inertia terms can be neglected. The variation of pressure gradient in circumferential and radial directions can be written as follows,

$$\frac{1}{r}\frac{\partial p}{\partial\theta}=\frac{1}{r^2}\frac{\partial}{\partial r}(r^2\tau_{r\theta})+\frac{1}{r}\frac{\partial\tau_{\theta\theta}}{\partial\theta}=\frac{\partial\tau_{r\theta}}{\partial r}+2\frac{\tau_{r\theta}}{r}+\frac{1}{r}\frac{\partial\tau_{\theta\theta}}{\partial\theta}, \quad (8)$$

$$\frac{\partial p}{\partial r}=\frac{1}{r}\frac{\partial}{\partial r}(r\tau_{rr})-\frac{\tau_{\theta\theta}}{r}+\frac{1}{r}\frac{\partial\tau_{r\theta}}{\partial\theta}=\frac{\partial\tau_{rr}}{\partial r}+\frac{1}{r}\frac{\partial\tau_{r\theta}}{\partial\theta}+\frac{\tau_{rr}-\tau_{\theta\theta}}{r}. \quad (9)$$

Now, the concept of energy gradient is employed to characterize the stability of viscoelastic flows (Dou, 2006a; Dou, 2006b; Dou, 2007). When the kinetic energy is negligible, the ratio of the *energy gradients* in transverse direction with that in streamwise direction becomes the ratio of *pressure gradients* in two directions,

$$K=\frac{\partial E/\partial n}{\partial H/\partial s}=\frac{\dfrac{\partial p}{\partial r}}{\dfrac{1}{r}\dfrac{\partial p}{\partial\theta}}=\frac{\dfrac{\partial\tau_{rr}}{\partial r}+\dfrac{1}{r}\dfrac{\partial\tau_{r\theta}}{\partial\theta}+\dfrac{\tau_{rr}-\tau_{\theta\theta}}{r}}{\dfrac{\partial\tau_{r\theta}}{\partial r}+2\dfrac{\tau_{r\theta}}{r}+\dfrac{1}{r}\dfrac{\partial\tau_{\theta\theta}}{\partial\theta}}, \quad (10)$$

which is a function of the coordinates in the flow domain. Here, $E=p+\frac{1}{2}\rho V^2$, is the total mechanical energy per unit volume fluid; H is the energy loss per unit volume fluid along the streamwise direction. For Newtonian fluid, H is the energy loss due to viscous friction along the streamwise direction. For viscoelastic fluid, it is seen from Eq. (9) and Eq. (10) that it is related to the variation of normal elastic stress $\frac{1}{r}\frac{\partial\tau_{\theta\theta}}{\partial\theta}$.

From the theory (Dou, 2006a; Dou, 2006b), the magnitude of K is an indication of instability. The stability of the flow depends on the maximum of K in the flow field, K_{max}. When the value of K_{max} in the flow field is larger than a critical value, the instability is expected to set in. In particular, if K_{max} tends to infinite, the flow is certainly unstable. For example, at the inflection point in Newtonian flow where the rate of energy loss $\partial H/\partial s$ is zero, the flow is sufficiently unstable. For viscoelastic flow, if there is an inflection point on the velocity profile, there must be a point on the velocity profile where $\frac{\partial\tau_{r\theta}}{\partial r}+2\frac{\tau_{r\theta}}{r}$ (Newtonian stress for given velocity profile) is zero. If $\frac{1}{r}\frac{\partial\tau_{\theta\theta}}{\partial\theta}$ is very small around this point, the energy loss along the streamline would be $\frac{\partial H}{\partial S}=\frac{1}{r}\frac{\partial p}{\partial\theta}=\frac{\partial\tau_{r\theta}}{\partial r}+2\frac{\partial\tau_{r\theta}}{r}+\frac{1}{r}\frac{\partial\tau_{\theta\theta}}{\partial\theta}\approx 0$. Thus, K_{max} is infinite from Eq. (10), and the flow must be unstable in this case. Generally, the critical value of K_{max} is a function of the curvature of streamlines. For flows with different wall curvature, the critical value of K_{max} takes different value.

For flows around a cylinder, the elastic stress gets its maximum at the cylinder surface. As we know, along the cylinder surface, the stresses are only related to the velocity gradient $\frac{\partial u_\theta}{\partial r}$, resembling the straight boundary layer flow case (Dou and Phan-Thien, 1999; Dou and Phan-Thien, 2007),

$$\tau_{\theta\theta}=2\lambda\beta\eta_0\left(\frac{\partial u_\theta}{\partial r}\right)^2,\quad \tau_{r\theta}=\beta\eta_0\left(\frac{\partial u_\theta}{\partial r}\right),\quad \tau_{rr}=0. \quad (11)$$

At the cylinder surface, $\frac{\partial\tau_{rr}}{\partial r}$ is very small. Thus, along the cylinder surface, Eq. (9) reduces to,

$$\frac{\partial p}{\partial r}=\frac{1}{r}\frac{\partial\tau_{r\theta}}{\partial\theta}-\frac{\tau_{\theta\theta}}{r}. \quad (12)$$

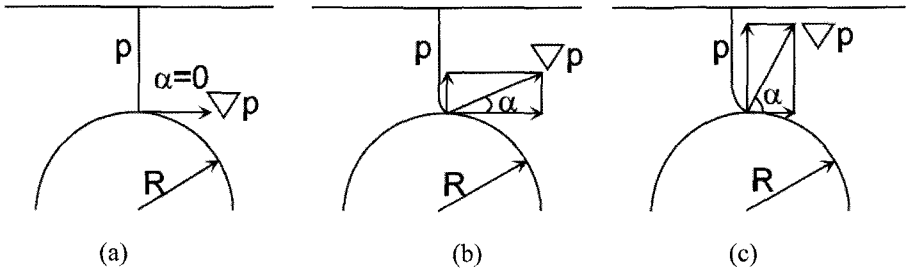

Fig. 3. Isobar of pressure and the direction of pressure gradient on the top of cylinder (K=arc tan α). (a) Newtonian flow, (b) Viscoelastic flow with low De, (c) Viscoelastic flow with high De.

With the increase of De, $\frac{\tau_{\theta\theta}}{r}$ becomes larger than $\frac{1}{r}\frac{\partial \tau_{r\theta}}{\partial \theta}$. When De is high, $\frac{1}{r}\frac{\partial \tau_{r\theta}}{\partial \theta} << \frac{\tau_{\theta\theta}}{r}$. Therefore, at the cylinder surface, Eq. (10) can be written as

$$K = \frac{\frac{1}{r}\frac{\partial \tau_{r\theta}}{\partial \theta} - \frac{\tau_{\theta\theta}}{r}}{\frac{\partial \tau_{r\theta}}{\partial r} + 2\frac{\tau_{r\theta}}{r} + \frac{1}{r}\frac{\partial \tau_{\theta\theta}}{\partial \theta}}. \tag{13}$$

If the stresses in above equation are normalized by a characteristic shear stress, it can be re-written as,

$$K = \frac{\frac{1}{r}\frac{\partial \bar{\tau}_{r\theta}}{\partial \theta} - De\frac{\bar{\tau}_{\theta\theta}}{r}}{\frac{\partial \bar{\tau}_{r\theta}}{\partial r} + 2\frac{\bar{\tau}_{r\theta}}{r} + De\frac{1}{r}\frac{\partial \bar{\tau}_{\theta\theta}}{\partial \theta}}. \tag{14}$$

Thus, it can be seen from above equation that K is a function of the Deborah number De for creeping viscoelastic flows. With the increase of De, the value of K increases since $De\frac{\bar{\tau}_{\theta\theta}}{r} >> De\frac{1}{r}\frac{\partial \bar{\tau}_{\theta\theta}}{\partial \theta}$, generally. When the value of K exceeds its critical value, the instability sets in. The physical meaning of K there is the direction of the pressure gradient, as shown in Fig. 3.

When an inflection point in the velocity profile appears, $\frac{\partial \tau_{r\theta}}{\partial r} + 2\frac{\tau_{r\theta}}{r}$ tends to zero near this point since this term is only related to Newtonian behaviour. If an inflection point is located near x=0, the value of K is very large from Eq. (10) owing to $\frac{1}{r}\frac{\partial \tau_{\theta\theta}}{\partial \theta} \sim 0$ at the plane near x=0 (not exactly at x=0 since $\tau_{\theta\theta}$ is not symmetrical with x=0 due to the convective (memory) terms in the constitutive equation). In this case, the flow tends to be unstable from the energy gradient theory (Dou, 2006a; Dou, 2006b). From the simulation results of an Oldroyd-B fluid, an inflection point appears at De=0.6, the flow may become unstable at this De number. However, as mentioned before, the critical value of De is a function of the curvature or the aspect ratio h/R. The critical value of De_c=0.6 is only for Oldroyd-B fluid and aspect ratio h/R=2. For the criterion used for different value of aspect ratio h/R, an expression will be derived in the next section.

The mechanism of instability can be described as follows. At low De, the pressure gradient due to $\frac{\tau_{\theta\theta}}{r}$ is not significant. With increasing De, this pressure gradient can be large near the cylinder surface. It, in turn, affects the u_θ distribution along the radial direction in such a way that the fluid particles in the thin shear layer near the cylinder surface are retarded by the radial pressure gradient. On other hand, the radial pressure gradient will drive a secondary flow in the radial direction, and result in an increase of the normal velocity u_r in the layer. Thus, the velocity component u_θ will decrease owing to mass conservation in the layer and a reduced velocity gradient will be produced. As such, at high De, the radial pressure gradient tends to lead to an inflection on the u_θ profile (Fig. 2), leading to flow instability according a newly developed theory (Dou, 2006a; Dou, 2006b). Therefore, it can be drawn that the flow instability at high De is due to the pressure distortion in the shear layer caused by the normal stress development along the cylinder surface (Eq. (10)).

McKinley *et al.* (1993) showed experimentally that the instability appeared in the cylinder wake, near the rear stagnation point and convected downstream. Larson (1992) thought that may be due to the extensional wake. We demonstrated by simulation that the origin of the physical instability is in the shear region on the cylinder, rather than in the wake itself (Dou and Phan-Thien, 2007). The instability is not initially generated in the extensional wake, but

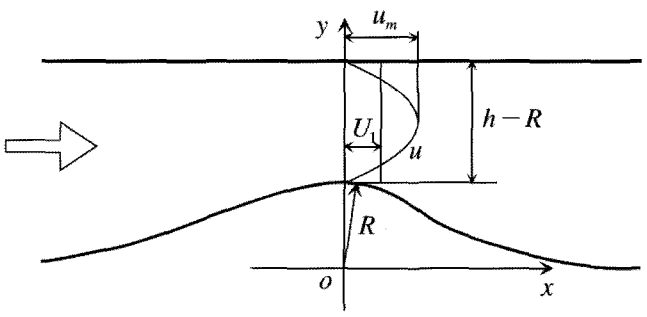

Fig. 4. Schematic of flow passage with a curved wall.

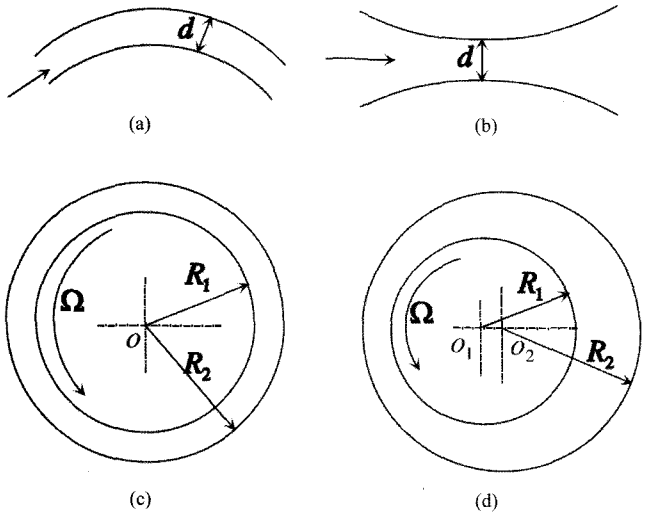

Fig. 5. Diagram of various geometry of planar shear instabilities. (a) Bend, (b) Throat, (c) Taylor-Couette flow, (d) Eccentric rotating cylinders.

is produced by normal stress on the cylinder due to elasticity, and the disturbance inducing instability is convected downstream into the wake. The instability on the cylinder is shear induced. These analyses are in agreement with the finding from experiment by Byars (1996). The behaviour of instability is the same as that in a pipe with a curved wall (Fig. 4). A few flow problems like flows in bends, throats, Taylor-Couette flow, and flow in eccentric rotating cylinders have the same types of shear-induced instabilities (Fig. 5).

In summary, viscoelastic flow instability transition takes place at a critical *De* number, which is generated by the pressure gradient in the cross-flow direction of shear flows, produced by the combined effects of the normal stress and the streamline curvature. It is expected that when the pressure gradient in the cross-flow direction is beyond a certain critical value, the inflection point in the velocity distribution would be generated and the instability sets in.

4.2. Criterion of instability in curved shear flows

In this section, we give a criterion for correlating the critical condition with different values of aspect ratio *h/R*. From the above discussion, it is understood that the instability is induced by the increase of elastic stress $\frac{\tau_{\theta\theta}}{r}$ with the increase of *De*, which generates large radial pressure gradient on the cylinder surface. From Eq. (12), the radial pressure gradient is mainly composed of two parts: $\frac{1}{r}\frac{\partial \tau_{r\theta}}{\partial \theta}$ and $\frac{\tau_{\theta\theta}}{r}$. As discussed before, when *De* is low, the elastic stress $\frac{\tau_{\theta\theta}}{r}$ is not large and $\frac{\partial p}{\partial r}$ is mainly generated from the shear stress $\frac{1}{r}\frac{\partial \tau_{r\theta}}{\partial \theta}$. When *De* is high, $\frac{\partial p}{\partial r}$ is mainly produced from the normal stress $\frac{\tau_{\theta\theta}}{r}$. With the increase of *De* from zero, $\frac{1}{r}\frac{\partial \tau_{r\theta}}{\partial \theta}$ gradually plays less role, and $\frac{\tau_{\theta\theta}}{r}$ gradually plays large role. In instability initiation, $\frac{\tau_{\theta\theta}}{r}$ can be expressed with an fraction of the pressure gradient $\frac{\partial p}{\partial r}$. When this part is smaller than a critical value, the flow is stable. It can be presumed that the relative magnitude of these two terms ($\frac{1}{r}\frac{\partial \tau_{r\theta}}{\partial \theta}$ and $\frac{\tau_{\theta\theta}}{r}$) can be used to correlate the critical condition for the instability with variation of *R/h*. Therefore, assuming that the ratio of the magnitudes of two terms is constant at the critical condition, the stability condition can be written as,

$$\frac{\tau_{\theta\theta}}{r} < \text{constan} \cdot \frac{1}{r}\frac{\partial \tau_{r\theta}}{\partial \theta}. \tag{15}$$

Here, it is assumed that Eq. (15) is suitable for different values of aspect ratio *h/R*. In other words, *the portion of* $\frac{\tau_{\theta\theta}}{r}$ *taking in the pressure gradient* $\frac{\partial p}{\partial r}$ *is the same for all the values of h/R at the critical condition.* Thus, in the next section, it is able to scale the critical condition versus the aspect ratio.

At the cylinder surface, the streamline is along the cylinder surface, $\frac{\tau_{\theta\theta}}{r} \sim \frac{\tau_{\theta\theta}}{R}$, and $\frac{1}{r}\frac{\partial \tau_{r\theta}}{\partial \theta} \sim \frac{\tau_0}{L_x}$. Here, τ_0 is a characteristic shear stress expressed by the shear rate and fluid viscosity (η_0), and L_x is a characteristic length in the streamwise direction. Since the cylinder surface is the most dangerous position for instability initiation, a stability criterion for *shear* flows of viscoelastic fluids is proposed as follow, referring to Eq. (15),

$$\frac{\tau_{\theta\theta}}{R} < A\frac{\tau_0}{L_x}, \tag{16}$$

where A is a constant (A takes different value for different constitutive models), which represents the critical condition for instability, and $\tau_{\theta\theta}$ is the normal stress in the shear layer on the cylinder surface (or curved wall surface) on the plane $x=0$, and R is the radius of the cylinder; and $\frac{\tau_{\theta\theta}}{r}$ gets its maximum at the surface of the cylinder. The characteristic length L_x is taken as the relaxation length in the streamwise direction, based on average velocity U_1, similar to that in Pakdel and McKinley (1996),

$$L_x = \lambda_1 U_1. \tag{17}$$

Using this in Eq. (16) results in

$$\frac{\tau_{\theta\theta}}{\tau_0}\frac{\lambda_1 U_1}{R} < A. \tag{18}$$

This criterion agrees with McKinley *et al.* (1996)'s,

derived using an analogy to the Görtler number. In this study, we consider the pressure gradient in the cross-flow direction generated by elastic normal stress to result in the instability. In both, the elastic instability is initiated by elastic normal stresses and streamline curvature effects. It is pointed out that Eq. (16) is a criterion for general shear flows with curvature, not simply specific to the cylinder problem. McKinley *et al.* (1996) thought that their criterion applies to both shear and extensional flows.

Recently, Groisman and Steinberg (2000) found that, at a large critical Deborah number, the behaviour of viscoelastic flows is similar to that of turbulence and named this type of flows as "elastic turbulence." The critical Deborah number in viscoelastic flows plays a similar role to the critical Reynolds number in Newtonian flows; its estimation is of significance.

5. Critical Deborah number for the cylinder problem

For the cylinder problem, the characteristic stress τ_0 is defined by fluid viscosity and the shear rate, based on the average velocity U_1 at $x=0$,

$$\tau_0 = \eta_0 \frac{U_1}{L_1}, \tag{19}$$

where L_1 is a suitable length scale. U_1 may be estimated as

$$U_1 = \frac{Uh}{(h-R)}, \tag{20}$$

where $h-R$ is the gap width between the cylinder and the wall at $x=0$,and h is the channel half width. For moderate aspect ratio R/h (*i.e.* $R/h=0.5$), L_1 may be taken as the half width of the passage at $x=0$, *i.e.* $L_1=(h-R)/2$. At small values of R/h, the shear rate should be scaled with the cylinder radius R, not with $(h-R)/2$, and hence $L_1=R$. We propose a simple linear relation for the length scale ratio L_1/R,

$$L_1 = R\left(1-\frac{R}{h}\right). \tag{21}$$

When $h/R\to\infty$, $U_1\to U$ and $L_1\to R$. For $R/h=0.5$, $U_1=2U$ and $L_1=R/2$, thus $U_1/L_1=4U/R$. Therefore, the shear rate is higher in the gap for higher values of R/h. This is reasonable flow physics.

For still higher values of R/h (>0.50), the value of $(h-R)/R$ is small and the effects of the contraction and expansion should be taken into account. More importantly, the influence of the curvature on the cylinder side should be reduced. Here only $(h-R)/R\geq 1.0$ (*i.e.*, $R/h\leq 0.5$) is considered.

5.1. Oldroyd-B fluid

The stresses in the shear layer on the cylinder surface can be obtained by analytical solutions. For the Oldroyd-B and UCM models, the normal stress is given by (Dou and Phan-Thien, 1999),

$$\tau_{\theta\theta} = 2\lambda\beta\eta_0\dot{\gamma}^2, \tag{22}$$

where $\dot{\gamma}$ is the shear rate. We take $\dot{\gamma}\approx U_1/L_1$ here. Introducing Eq. (19)-(22) into Eq. (16), this allows the critical Deborah number for the Oldroyd-B fluid to be written as

$$De_c = \sqrt{\frac{A}{2\beta}}\left(1-\frac{R}{h}\right)^{\frac{3}{2}}. \tag{23}$$

Using the simulated results, $De_c=0.6$ for $h/R=2$ and $\beta=0.41$, it is found that $A=2.3615$. Thus, the critical De can be written as

$$De_c = \frac{1.09}{\sqrt{\beta}}\left(1-\frac{R}{h}\right)^{\frac{3}{2}}. \tag{24}$$

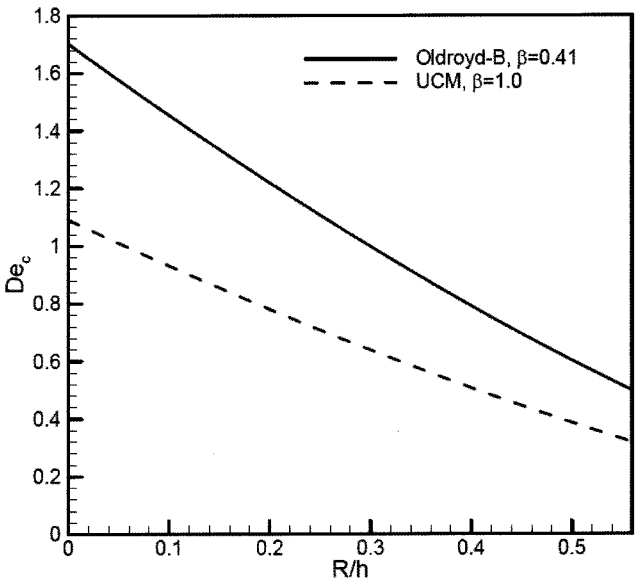

Fig. 6. Critical De number versus the aspect ratio for Oldroyd-B ($\beta=0.41$) and UCM fluids.

The critical Deborah number for Oldroyd-B ($\beta=0.41$) and UCM fluids versus the aspect ratio h/R are plotted in Fig. 6. The scaling $O(\beta^{-1/2})$ is also found in cone-and-plate flow (Phan-Thien, 1985; Olagunju and Cook, 1993). When β tends to zero, the (Newtonian) flow is unconditionally stable, in agreement with the linear stability analysis of cone-and-plate flow (Phan-Thien, 1985), Poiseuille flows (Sureshkumar *et al.*, 1999) and torsional flows between parallel plates (Avagliano and Phan-Thien, 1998, 1999). Experiments by Groisman and Steinberg (1998) confirmed the dependence of critical instability on viscosity ratio of the fluid.

For unbounded flow past a cylinder, $h/R\to\infty$, the critical Deborah number is

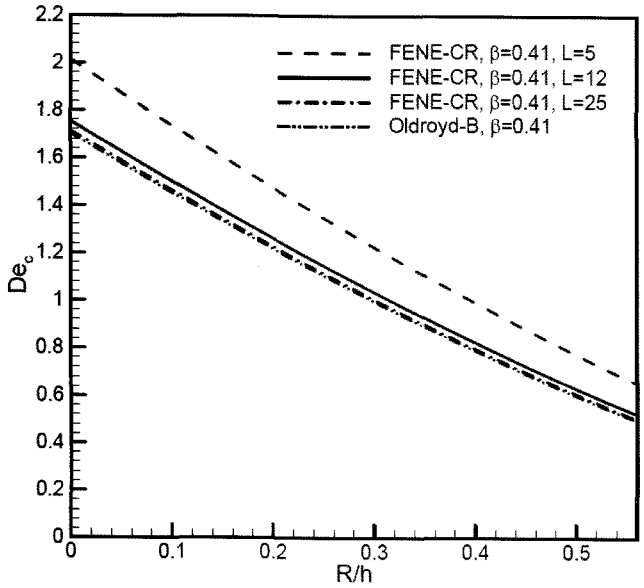

Fig. 7. Critical *De* number versus the aspect ratio for FENE-CR fluids (β=0.41, and L=5, L=12, L=25) and Oldroyd-B fluid (β=0.41).

$$De_c = \frac{1.09}{\sqrt{\beta}}. \tag{25}$$

For the MIT Boger fluid, β=0.41, a critical Deborah number of De_c=1.70 is obtained for an isolated cylinder in an infinite domain.

5.2. FENE-CR fluid

For the FENE-CR model, the normal stress is given by the analytical solution:

$$\tau_{\theta\theta} = 2\lambda\beta\eta_0\dot{\gamma}^2\frac{2(L^2-3)}{L^2}\left[1+\sqrt{1+8(\lambda\dot{\gamma})^2\frac{L^2-3}{L^4}}\right]^{-1}, \tag{26}$$

where $\dot{\gamma}$ is the shear rate for the shear flow in the passage between the cylinder and the channel wall at plane x=0. Again, as in the Oldroyd-B fluid we take $\dot{\gamma}=U_1/L_1$. Note that the FENE-CR model includes the Oldroyd-B or the UCM model depending on the value of β (with $L\to\infty$). For the FENE-CR model, the critical Deborah number can be derived in a similar way. The critical *De* for the FENE-CR fluid is

$$De_c = \sqrt{\frac{AL^2}{4\beta(L^2-3)}}\left(1-\frac{R}{h}\right)^{\frac{3}{2}}\left[1+\sqrt{1+8De_c^2\left(1-\frac{R}{h}\right)^{-4}\frac{L^2-3}{L^4}}\right]^{\frac{1}{2}},$$

giving

$$De_c = \left(1-\frac{R}{h}\right)^{\frac{3}{2}}\sqrt{\frac{AL^2}{2\beta(L^2-3)}\left[1+\frac{A}{\beta L^2}\left(1-\frac{R}{h}\right)^{-1}\right]}. \tag{27}$$

Assuming the same constant A=2.3615 as in the Oldroyd-B fluid, this becomes,

$$De_c = 1.09\left(1-\frac{R}{h}\right)^{\frac{3}{2}}\sqrt{\frac{L^2}{\beta(L^2-3)}\left[1+\frac{2.3615}{\beta L^2}\left(1-\frac{R}{h}\right)^{-1}\right]}. \tag{28}$$

When the value of L tends to infinite, the FENE-CR fluid reduces to Oldroyd-B fluid. For a unbounded cylinder, $h/R\to\infty$, the critical Deborah number is

$$De_c = \frac{1.09}{\sqrt{\beta}}\sqrt{\frac{L^2}{(L^2-3)}\left[1+\frac{2.3615}{\beta L^2}\right]}. \tag{29}$$

The critical Deborah number versus the aspect ratio h/R for FENE-CR (β=0.41, and L=5, L=12 and L=25) fluids, as well as the Oldroyd-B fluid, is shown in Fig. 7. Compared to the Oldroyd-B fluid, the instability of the FENE-CR fluid is delayed and a higher De_c is obtained, which increases with decreasing L. This is due to the shear thinning of the first normal stress coefficient Ψ_1. These effects of β and L are in agreement with those of torsional flows (Byars *et al.*, 1994; Avagliano and Phan-Thien, 1998, 1999). Both the Oldroyd-B and the FENE-CR models have been used in modelling of constant viscosity Boger fluids. In some cases, simulations with the Oldroyd-B model also yielded good results compared to experiments. From Fig. 7, it is seen that the critical Deborah numbers for instability initiation are almost the same for the FENE-CR fluid (L=25) and Oldroyd-B fluid. This is because the shear property of this fluid at large L (L^2=625) and moderate shear rates is not different from that of the Oldroyd-B fluid. The difference of these two models is mainly in the extensional properties. Therefore, if the flow is dominated by shear and the shear rate is not very large, the Oldroyd-B

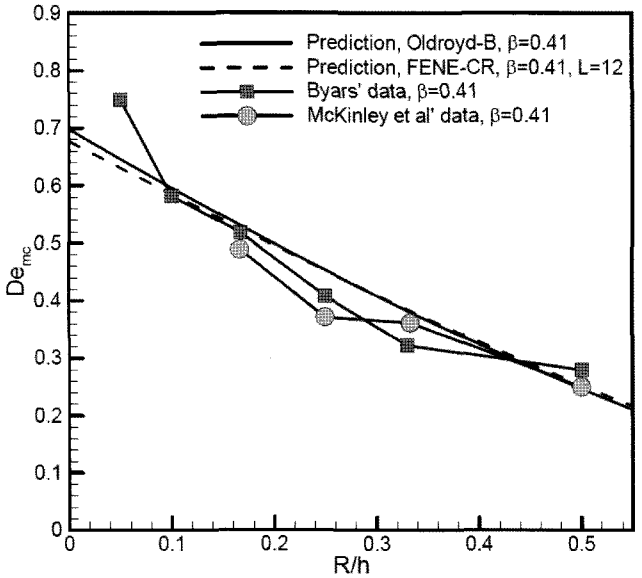

Fig. 8. A comparison of the present criterion with experimental data of Byars (1996) and McKinley *et al.* (1993). Both sets of data are taken from Byars (1996). Here, R/h=0 (or h/R=∞) represents the case of an unbounded cylinder.

model should be a good model.

It may be more appropriate to express the effect of elasticity using a shear rate-dependent Deborah number:

$$De_s = \frac{\Psi_1(\dot{\gamma}_s)}{2\eta_m(\dot{\gamma}_s)}\dot{\gamma}_s = \lambda\dot{\gamma}_s\frac{2(L^2-3)}{L^2}\left[1+\sqrt{1+8(\lambda\dot{\gamma}_s)^2\frac{L^2-3}{L^4}}\right]^{-1}, \quad (30)$$

where $\dot{\gamma}_s = U/R$. McKinley *et al.* (1993) used another shear rate-dependent Deborah number, here expressed as De_m which is related to De_s as follows,

$$De_m = \frac{\Psi_1(\dot{\gamma}_s)}{2\eta(\dot{\gamma}_s)}\dot{\gamma}_s = \beta De_s$$

A comparison of the present criterion with experimental data of Byars (1996) and McKinley *et al.* (1993) is shown in Fig. 8. The abscissa in Fig. 8 is the aspect ratio R/h of the flow geometry; the ordinate is De_{mc} which is the critical value of De_m, expressed by Eq. (31). The predictions are for the Oldroyd-B fluid (β=0.41) and the FENE-CR (β=0.41 and L=12) fluid. The critical Deborah number at constant shear rate, De_c, is first calculated using either Eq. (24) (for Oldryd-B fluid) or Eq. (28) (for FENE-CR fluid), then the value of De_{mc} is converted from the value of De_c using Eqs. (30) and (31), in order to compare with McKinley et al's data. It is noticed that $De = \lambda\dot{\gamma}_s$ and De_s is a function of De from Eq. (30).

The predicted critical Deborah number De_{mc} for the FENE-CR model and Oldroyd-B model is about the same for moderate values of R/h. This is because the shear rate-dependent Deborah number, De_m, represents the effect of shear, and both models have roughly the same shear behaviour at moderate shear rate.

The good agreement between the prediction and experiments confirms that the proposed criterion is valid, although it may be semi-empirical. This is due to the fact that the instability is a shear-induced one, which is then convected to the wake leading to the wake instability. This instability is originated on the top of the cylinder and induced by the velocity inflection point, which occurs in the very thin layers on the cylinder, and is difficult to locate either by numerical simulations or by experiments.

McKinley *et al.* (1996)'s results from the linear stability calculations (using the similarity solution which is valid in the stagnation region) did not fit the scaling well enough. This is an indication that a consideration of the flow in the wake region may not be helpful.

Byars (1996)' measurements close to the cylinder (for R/h =0.50) showed that the instability also exists along the cylinder *upstream* of the rear stagnation point. The angular extent ($\pm\theta$ in Fig. 1) of the instability increases linearly as the Deborah number increases above De_c. For the case of $De_m - De_{mc}$=0.27, the instability extends 45 degree upstream of the rear stagnation point, while for higher $De_m - De_{mc}$ the instability has been observed as far as 60 degree upstream. This clearly showed that the origin of the instability is upstream of the rear stagnation point, not in the wake.

Finally, we should give a remark about the difference between pure elastic instability and inertia instability. The influence of elasticity on these two types of instabilities may be different since these two types of instabilities are dominated by different mechanisms. One should not confuse inertia instability and elastic instability. For flows of Newtonian fluids, there is always a critical Re number ($Re \neq 0$) beyond which the flow is unstable. In this type of flow, viscosity damps the disturbance and stabilizes the flow, generally, due to large viscosity leading to high energy loss (Dou, 2006a; Dou 2006b). The instability in this case is due to the inertia (kinetic energy). For this case, elasticity may enhance the stability. For example, elastic force may resist the roll up instability in free shear layer. However, for the case of creeping flows of viscoelastic fluids, the flow is stable for low De, but it is unstable for high De number due to combined influences of elastic normal stress and streamline curvature. This means that elasticity destabilizes the flow for this case, as studied in this study.

Kumar and Homsy (1999) studied the effect of elasticity on the instability of straight free shear flow at a relative large Re. Their research indicates that for large elastic number $E=De/Re$ and the maximum dumbbell extensibility L, the addition of polymers can inhibit the instabilities leading to turbulence in free shear layers, by interfering with the roll-up process of inflectional velocity profiles. As we know, for pure elastic instability occurring in creeping flows of viscoelastic fluids, the instability is nothing to do with the inertia. The effect of elasticity on instability of flow along curved surfaces, which is due to effect of curvature, is different from that in free shear flows. There is a key difference about the instability in these flows. For inertial instability in free shear flows or straight boundary layer flows, it may be true that elasticity delay instability by resist the rolling process of the vortices. For creeping elastic flow along curved surface at $Re \approx 0$, elasticity amplifies the instability by generating a pressure gradient normal to the wall on the curved surfaces.

For boundary layer flows of Newtonian fluids, the occurrence of inflectional velocity profile is caused by the streamwise pressure gradient which is produced by the deceleration at high Re (Schlichting and Gersten, 2000; White, 1991). For boundary layer flows of viscoelastic fluids, the occurrence of inflectional velocity profile is induced by the vertical pressure gradient which is generated by the elastic normal stress on a curved wall (Dou and Phan-Thien, 2007). Although the processes and leading factors for the velocity inflection generation are different from each other for the two kind of flows, the result is the same that there is an increasing vertical velocity leading to a secondary flow and the flows become unstable. At sufficiently high De number, the secondary flow driven by the normal stress can produce a growing oscillatory response

to the small initial disturbance. In summary, the radial secondary flow induced by normal stress which may be difficult to identify is the reason of instability. At high *De* number, this radial secondary flow will inevitably result in velocity inflection owing to the limitation of mass flow conservation. Joo and Shaqfeh (1992), McKinley *et al.* (1996), and Groisman and Steinberg (1998) use criteria for the instability initiation. In this study, a more practical criterion for flow instability under viscoelastic stress is given.

6. Conclusions

This report attempts to derive a viscoelastic instability criterion for the flow passing a confined cylinder. The critical Deborah number is given for different differential constitutive models. The study is based on numerical results and the understanding of the physical problems at high *De* number. The main conclusions of this study are as follows:

① The precursor of the instability is the velocity inflection at a critical *De* number. The pressure distortion near the cylinder due to the combined effects of normal stress and streamline curvature induces a secondary flow and results in the inflection in the velocity owing to mass conservation.

② A criterion for the shear viscoelastic instability is proposed based on the analysis of the energy (pressure) gradient. This criterion is consistent with that proposed by McKinley *et al.* (1996).

③ The critical Deborah number is of $O(\beta^{-1/2})$. When β tends to zero, the flow is unconditionally stable.

④ The critical *De* number for the FENE-CR model is higher than that of the Oldroyd-B model. The shear thinning of the first normal stress coefficient Ψ_1 delays the onset of instability.

⑤ The critical Deborah number given by the criterion (with semi-empirical treatment) agrees well with available experimental data.

⑥ The energy gradient theory has been successful for both Newtonian and viscoelastic flows. It seems that K is a universal function for instability.

Acknowledgment

The authors are grateful to Dr. J. Byars for making available his experimental data. The authors also acknowledge helpful comments from Prof. R. I. Tanner.

References

Avagliano, A. and N. Phan-Thien, 1998, Torsional flow: effect of second normal stress difference on elastic instability in a finite domain, *J. Fluid Mech.* **359**, 217-237.

Avagliano, A. and N. Phan-Thien, 1999, Torsional flow stability of highly dilute polymer solutions, *J. Non-Newt. Fluid Mech.* **84**, 19-44.

Bird, R.B., R.C. Armstrong and O. Hassager, 1987, Dynamics of polymeric liquids, vol.1: fluid mechanics, 2nd ed.,Wiley, New York.

Byars, J. A., A. Öztekin, R. A. Brown and G. H. McKinley, 1994, Spiral instabilities in the flow of highly elastic fluids between rotating parallel disks, *J. Fluid Mech.* **271**, 173-218.

Byars, J. A., 1996, Experimental characterization of viscoelastic flow instabilities, Ph.D thesis, MIT, Cambridge, MA 02139, USA.

Coala, A. E., Y. L.Joo, R. C. Armstrong and R. A. Brown, 2001, Highly parallel time integration of viscoelastic flows, *J. Non-Newt. Fluid Mech.* **100**, 191-216.

Dou, H-S., 2004, Viscous instability of inflectional velocity profile, Proc.of the foruth international conference on fluid mechanics, Ed. by F. Zhuang and J. Li, Tsinghua University Press & Springer-Verlag, Beijing, 76-79.

Dou, H-S., 2006a, Mechanism of flow instability and transition to turbulence, *Inter. J. of Non-Linear Mech.* **41**, 512-517. http://arxiv.org/abs/nlin.CD/0501049.

Dou, H-S., 2006b, Physics of flow instability and turbulent transition in shear flows, Technical report, National university of singapore, 2006. http://www.arxiv.org/abs/physics/0607004. Also as part of the invited lecture: H.-S. Dou, Secret of Tornado, International workshop on geophysical fluid dynamics and scalar transport in the tropics, NUS, Singapore, 13 Nov. - 8 Dec., 2006.

Dou, H-S., 2007, Three important theorems for flow stability, Proc. of the fifth international conference on fluid mechanics, Ed. by F. Zhuang and J. Li, Tsinghua University press & Springer-Verlag, Beijing, 56-70. http://www.arxiv.org/abs/physics/0610082.

Dou, H.-S., B. C. Khoo and K. S.Yeo, 2007, Instability of Taylor-Couette flow between concentric rotating cylinders, *Inter. J. Thermal Science*, accepted and in press, http://arxiv.org/abs/physics/0502069.

Dou, H.-S. and N. Phan-Thien, 1999, The flow of an Oldroyd-B fluid past a cylinder in a channel: adaptive viscosity vorticity (DAVSS-omega) formulation, *J. Non-Newt. Fluid Mech.* **87**, 47-73.

Dou, H.-S. and N. Phan-Thien, 2007, Viscoelastic flow past a confined cylinder: instability and velocity inflection, *Chemical Engineering Science* **62**, 3909-3929.

Groisman, A. and V. Steinberg, 1998, Mechanism of elastic instability in Couette flow of polymer solutions-experiment, *Phys. Fluids* **10**, 2451-2463.

Groisman, A. and V. Steinberg, 2000, Elastic turbulence in a polymer solution flow, *Nature* **405**, 53-55.

Huilgol, R. R. and N. Phan-Thien, 1997, Fluid mechanics of viscoelasticity: general principles, constitutive modelling and numerical techniques, Rheology series vol. 6, Elsevier, Amsterdam.

Hulsen, M. A., R. Fattal and R. Kupferman, 2005, Flow of viscoelastic fluids past a cylinder at high Weissenberg number: stabilized simulations using matrix logarithms, *J. Non-Newt. Fluid Mech.* **127**, 27-39.

Joo,Y. L. and E. S. G.Shaqfeh, 1992, A purely elastic instability in Dean and Taylor-Dean flow, *Phys. Fluids A* **4**, 524-543.

Kim, J. M., C. Kim, K. H. Ahn and S. J. Lee, 2004, An efficient iterative solver and high-resolution computations of the Oldroyd-B fluid flow past a confined cylinder, *J. Non-Newt. Fluid Mech.* **123**, 161-173.

Kumar, S. and G. M. Homsy, 1999, Direct numerical simulation of hydrodynamic instabilities in two-and three-dimensional viscoelastic free shear layers, *J. Non-Newt. Fluid Mech.* **83**, 249-276.

Larson, R. G., 1992. Instabilities in viscoelastic flows, *Rheol. Acta* **31**, 213-263.

Larson, R. G., E. S. G. Shaqfeh and S. J. Muller, 1990, A purely elastic instability in Taylor-Couette flow, *J. Fluid Mech.* **218**, 573-600.

McKinley, G. H., R. C. Armstrong and R. A. Brown, 1993, The wake instability in viscoelastic flow past confined circular cylinders, *Phil. Trans. R. Soc. Lond. A* **344**, 265-304.

McKinley, G. H., P. Pakdel and A. Öztekin, 1996, Rheological and geometric scaling of purely elastic flow instabilities, *J. Non-Newt. Fluid Mech.* **67**, 19-47.

Olagunju, D. O. and L. P. Cook, 1993, Linear-stability analysis of cone and plate flow of an Oldroyd-B fluid, *J. Non-Newt. Fluid Mech.* **47**, 93-105.

Oliveira, P. J. and A. I. P. Miranda, 2005, A numerical study of steady and unsteady viscoelastic flow past bounded cylinders, *J. Non-Newt. Fluid Mech.* **127**, 51-66.

Pakdel, P. and G. H. McKinley, 1996, Elastic instability and curved streamlines, *Phys. Rev. Lett.* **77**, 2459-2462.

Phan-Thien, N., 1985, Cone and plate flow of the Oldroyd-B fluid is unstable, *J. Non-Newt. Fluid Mech.* **17**, 37-44.

Schlichting, H. and K. Gersten, 2000, Boundary layer theory, Springer, 8th Ed., Berlin, 415-494.

Shaqfeh, E. S. G., 1996, Purely elastic instabilities in viscoelastic flows, *Annu. Rev. Fluid Mech.* **28**, 129-186.

Shiang, A. H., A.Öztekin and D. Rockwell, 2000, Hydroelastic instabilities in viscoelastic flow past a cylinder confined in a channel, *Exp. Fluids* **28**, 128-142.

Smith, M. D., R. C. Armstrong, R. A. Brown and R. Sureshkumar, 2000, Finite element analysis of stability of two-dimensional viscoelastic flows to three-dimensional perturbations, *J. Non-Newt. Fluid Mech.* **93**, 203-244.

Sureshkumar, R., M. D. Smith, R. C. Armstrong and R. A. Brown, 1999, Linear stability and dynamics of viscoelastic flows using time-dependent numerical simulations, *J. Non-Newt. Fluid Mech.* **82**, 57-104.

White, F. M., 1991, Viscous fluid flow, McGraw-Hill, New York, 2nd Ed., 335-393.

Wilson, H. J., 2006, Instabilities and constitutive modelling, *Phil. Trans. R. Soc. A* **364**, 3267-3283.